A Series of Thienylene/Phenylene-Based Polymers Functionalized with Electron-Withdrawing or -Donating Groups: Synthesis and Characterization

J. M. Xu, S. C. Ng,* and H. S. O. Chan

Department of Chemistry, National University of Singapore, Singapore 119260

Received August 29, 2000; Revised Manuscript Received March 13, 2001

ABSTRACT: A series of polymers comprising alternating phenylene and thienylene repeating units and with electron-donating or -withdrawing groups attached on thienylene units, i.e., poly[1,4-bis(3-X-2,5-thienylene)phenylene-*alt*-2,5-dioctyl-1,4-phenylene] (PBTX, X = OMe, H, Cl, Br, CN), has been synthesized and characterized. These polymers are highly fluorescent, among which PBTH shows the highest solution quantum yield, up to 94% relative to quinine sulfate. The absorption and emission peak wavelengths of PBTOMe are bathochromically shifted and band gap (E_g) is lowered by the presence of electron-donating OMe group, in comparison with PBTH. The influence of electron-withdrawing groups, Br, Cl, and CN, on the absorption peak wavelength and E_g, on the other hand, is not so great. Nevertheless, the film of PBTCN shows an emission maximum near to that of PBTOMe due to the strong interchain interactions. The band structures as deduced from electrochemistry give information supporting the optical measurements. The IP of PBTOMe is decreased but EA is increased, resulting in a lower band gap than that of PBTH. The electronic structures of PBTBr and PBTCl change slightly in comparison with PBTH, but both the IP and EA of PBTCN are greatly increased (by 0.5 eV), leading to an unchanged E_g. The changes in electronic structure make PBTOMe a suitable candidate as an active layer in LED device, as it should favor a balanced electron and hole injection, despite its moderate quantum yield. PBTCN can be used as an excellent ETL material in multilayer devices as its EA is even higher than that of CN−PPV. The polymers are dopable by $FeCl_3$ and I_2 except for PBTCN, in agreement with electrochemical results. PBTH shows a good conductivity up to 4 S cm^{-1} when doped by $FeCl_3$. The doped samples are examined using XPS and the formation of charge-transfer complex is suggested. The oxidization of both the S and O atoms in $FeCl_3$-doped PBTOMe is also supported by XPS.

Introduction

The application of conjugated polymers as active layers in light-emitting diodes (LEDs) with low turn-on voltages started nearly a decade ago, during which time conjugated polymers such as poly(*p*-phenylene vinylene),[1,2] poly(*p*-phenylene),[3,4] polythiophene,[5,6] and their derivatives or copolymers have been found to be the candidates as luminescent materials. The emission color, emission efficiency, driving voltage, and long-term stability have been the focuses of LED device research. Although these parameters are greatly influenced by device configurations and operation conditions,[7,8] it is of primary importance to synthesize polymers with the expected properties. Polymer substitution with different functional groups has been found to be one of the ways to achieving this aim, as the electronic structure and correspondingly, the optical property of the polymers can be adjusted. In addition, modification of polymer structure also leads to the adjusting of solubility, processability, stability and other physicochemical properties. For example, CN−PPV [poly(2,5-dihexoxyphenylene-8-cyano-*p*-phenylene vinylene)] was substituted by electron-donating (OR) and electron-withdrawing (CN) groups. E_g of CN−PPV is mainly determined by the effect of the alkoxy substituent, which also serves to promote solubility in $CHCl_3$ and thus ensure processability. The cyano substituent contributes to both the increase in electron affinity (EA) and ionization potential (IP).[9] As a result, CN−PPV is an excellent electron transport layer (ETL) as well as an efficient emissive material.

The EA of a polymer is crucial in the actual application of the polymer as an active material in LEDs. To achieve efficient electron injection, the cathode must be carefully chosen so that the barrier between cathode and polymer is not too high. As the EAs of common conjugated polymers are usually below 2.9 eV,[10] calcium, which has a low work function on the order of 2.9−3.0 eV, is preferred as a cathode. However, Ca is very active and has a negative effect on the long-term stability of devices. It is therefore very important to produce polymers of high electron affinity so that more stable metals, such as Al (work function 4.3−4.4 eV), can be used as cathodes, while device efficiency can be maintained. In this regard, if we use PPV derivatives as an example again, electron-withdrawing groups, such as CN, Br, Cl, and CF_3, have been incorporated into the PPV structure.[9,11−14] While CN−PPV shows excellent performance as both an emissive layer and ETL material, the CF_3-substituted polymer has a higher EA than PPV and emits at shorter wavelengths as expected, but its quantum yield is lower. It is thus more likely to be used as an ETL candidate in device application.

We have reported earlier the synthesis and characterization of polymers containing alternating phenylene and electron-donating group [alkyl (R) or alkylthio (SR)] functionlized thienylene/bithienylene (PBTBC$_n$, PBTC$_n$, PBTBSC$_n$ and PBTSC$_n$, n = 4, 8, and 12) repeating units.[15−19] These polymers are fluorescent, conducting, and thermally stable in the doped state. The influence of alkyl chain length, polymer backbone structure

* Corresponding author.

10.1021/ma0015018 CCC: $20.00
Published on Web 05/25/2001

modification and electron-donating ability of pendant chains had been noted and discussed. In addition, one of them, $PBTC_4$,[16] had been applied to the fabrication of LED device with Mg/In alloy (work function 3.7 eV) as a cathode. To make further investigation on the structure−property correlation and to synthesize novel materials which are highly fluorescent or with special properties for use in the fabrication of LED devices, we had synthesized and characterized a new series of regioregular polymers substituted by methoxy (OMe), hydrogen (H), chlorine (Cl), bromine (Br) and cyano (CN) groups, i.e., poly[1,4-bis(3-X-2,5-thienylene)phenylene-*alt*-2,5-dioctyl-1,4-phenylene] (PBTX, X = OMe, H, Cl, Br, CN).

Experimental Section

Materials. Diethyl ether (Et_2O, J. T. Baker, AR), nitromethane (Fisher, AR) and *N*,*N*-dimethylformamide (DMF, Merck, AR) were dried carefully prior to use. 1-Bromooctane (Merck), Ni(dppp)Cl_2 (Fluka), magnesium (Fluka), *N*-bromosuccinimide (NBS, Merk), anhydrous ferric chloride ($FeCl_3$, Riedel-deHane), butyllithium (BuLi, TCI), 1,2-dibromoethane (BDH), 1,4-dibromobenzene (Fluka), bromine (Merck), zinc dust (Fluka), cuprous chloride (CuCl, Fluka), cuprous cyanide (CuCN, Fluka), 3-methoxythiophene (Fluka), tributyltin chloride (Bu_3SnCl, Fluka), and iodine (I_2) for synthesis (Fisher) were used as received. Tetrabutylammonium tetrafluoroborate (Bu_4NBF_4, TCI) was dried under high vacuum at 60 °C for 24 h prior to use. Pd$(PPh_3)_2Cl_2$ was synthesized according to the literature.[20]

Instrumentation. ^{1}H NMR spectra were recorded on a 300 MHz Bruker ACF 300 FT-NMR spectrophotometer. The 75 MHz ^{13}C NMR spectra were obtained using the same instrument. Deuterated chloroform was used as solvent and tetramethylsilane (TMS) as the internal reference. EIMS and HRMS spectra were obtained using a micromass 7034E mass spectrometer. Elemental analyses of all the monomers and polymers were conducted at the NUS Microanalytical Laboratory on a Perkin-Elmer 240C elemental analyzer for C, H, and S determination. Halogen determinations were done either by ion chromatography or the oxygen flask method. Gel permeation chromatography (GPC) analyses were carried out using a Perkin-Elmer model 200 HPLC system with Phenogel MXL and MXM columns (300 mm × 4.6 mm ID, MW 100−100K and 5−500K, respectively) calibrated using polystyrene standards. THF was used as eluant, and the flow rate was 0.35 mL min^{-1}. FTIR spectra of the polymers and solid monomers dispersed in KBr disks, and of neat liquid of small molecules sandwiched between NaCl disks were recorded on a Bio-Red TFS 156 spectrometer. Solution phase and solid-state absorption and fluorescence spectrum measurements of the polymers were conducted on a Hewlett Parkard 8452A spectrophotometer and Shimadzu RF5000 fluorescence spectrophotometer, respectively. Dilute polymer solutions dissolved in spectrograde chloroform (10^{-5}−10^{-6} M) were used for analysis. Optical absorption from thin polymer films deposited onto indium tin oxide (ITO) coated glass plates was obtained on a Lamda 900 spectrophotometer. Thermogravimetry (TG) was conducted on a Du Pont Thermal Analyst 2100 system with a TGA 2950 thermogravimetric analyzer in air (75 mL min^{-1}) at a heating rate of 10 °C min^{-1} from room temperature to 1000 °C. Conductivity measurements were carried out on polymer pellets of known thickness using a four-point probe connected to a Keithley constant current source. XPS measurement of polymer powder or films (on ITO) was performed by means of a VG ESCA/SIMLAB MKII with a Mg Kα radiation source (1253.6 eV). The binding energies were corrected for surface charging by referencing to the designated hydrocarbon C(1s) binding energy as 284.6 eV. Spectrum deconvolutions were carried out using the Gaussian component with the same full width at half-maximum (fwhm) for each component in a particular spectrum. Surface elemental stoichiometries were obtained from peak area ratios corrected with the appropriate experimentally determined sensitivity factors.

Cyclic voltammetry of solution cast polymer films was carried out using an EG&G 273A potentiostat/galvanostat controlled by EG&G M270 research electrochemistry software and a three-electrode single compartment chemical cell consisted of an ITO glass plate as the working-electrode, a platinum wire as the counter electrode and a Ag/$AgNO_3$ (in 0.1 M acetonitrile) as the quasi-reference electrode [0.35 V vs saturated calomel electrode (SCE)] in a solution of 1 M Bu_4NBF_4 in acetonitrile under argon atmosphere. In situ electrochromism studies of polymers were conducted in a single-compartment, three electrode quartz cell comprising a film-coated ITO working electrode, a platinum counter electrode and a silver wire quasi-reference electrode using the potentiostat together with a Lamda 900 UV−vis−NIR spectrometer in the same electrolyte system as CV.

Synthesis. Synthesis of DBBTBX (X = OMe, H, Cl, Br, CN). The synthesis of 1,4-bis(2-thienyl)benzene (BTB), 1,4-bis(3,5-dibromo-2-thienyl)benzene (DBBTBBr), and 1,4-bis(3-bromo-2-thienyl)benzene (BTBBr) will be described elsewhere.[19]

General Procedure for the Preparation of 1,4-Bis(3-X-2-thienyl)benzene (BTBX, X = CN, Cl). BTBBr (2.80 g, 7.03 mmol) dissolved in dry DMF was transferred via a cannula into a 25 mL round-bottom flask which contained cuprous chloride or cyanide (CuX, X = CN, Cl, 21.0 mmol) and DMF (8 mL) under nitrogen. The mixture was stirred at 120 °C for 24 h, cooled to ambient temperature, and poured into a large quantity of (ca. 400 mL) ammonium aqueous solution (NH_4OH, 28−30%) and stirred overnight. Extracting with chloroform, washing with water thoroughly, drying, and removing solvent led to a pale yellow solid.

1,4-Bis(3-cyano-2-thienyl)benzene (BTBCN, X = CN). It was recrystallized from chloroform as a fluffy product (53.5% yield, mp 253−254 °C). EIMS *m/z* (relative intensity): 292 (M^+, 100%). HRMS: calculated for $C_{16}H_8S_2N_2$ (M^+), 292.0129; found, 292.0128. IR (cm^{-1}): 3092, 3043, 3017, 2234, 1635, 1543, 1499, 1429, 890, 833, 748, 648. ^{1}H NMR (ppm): 7.89 (4H, s), 7.39 (2H, d, J = 5.3 Hz), 7.32 (2H, d, J = 5.3 Hz). Anal. Calcd for $C_{16}H_8S_2N_2$: C, 65.75; H, 2.74; S, 21.92; N, 9.59. Found: C, 62.37; H, 1.79; S, 21.38; N, 7.83.

1,4-Bis(3-chloro-2-thienyl)benzene (BTBCl, X = Cl). It was recrystallized from $CHCl_3$−EtOH. (73% yield, mp 123−124 °C). EIMS *m/z* (relative intensity): 314 (M^+ + 4, 40), 312 (M^+ + 2, 90), 310 (M^+, 100%). HRMS: calculated for $C_{14}H_8S_2Cl_2$ (M^+), 309.9444; found, 309.9441. IR (cm^{-1}): 3104, 3043, 3017, 1635, 1541, 1493, 1458, 1348, 887, 829, 702, 615. ^{1}H NMR (ppm): 7.74 (4H, s), 7.28 (2H, d, J = 5.4 Hz), 7.01 (2H, d, J = 5.3 Hz). ^{13}C NMR (ppm): δ 135.41, 131.82, 129.40, 128.60, 124.04, 121.59. Anal. Calcd for $C_{14}H_8S_2Cl_2$: C, 54.02; H, 2.57; S, 20.58; Cl, 22.83. Found: C, 53.59; H, 1.64; S, 20.01; Cl, 23.07.

2-Tributylstannyl-3-methoxythiophene (TTOMe). 3-Methoxythiophene (1.0 mL, 10.0 mmol) was dissolved in ether (2 mL) in a 50 mL two-necked round-bottom flask under nitrogen and then BuLi (1.1 M in hexane, 9.1 mL, 10.0 mmol) was syringed in at 0 °C. After the mixture was stirred at room temperature for 2 h, it was cooled to 0 °C again, and a solution of Bu_3SnCl (3.25 g, 10.0 mmol) in ether (5 mL) was introduced. The reaction mixture was warmed to room temperature and stirred for 12 h and then cooled to ambient temperature and neutralized with NH_4Cl solution. A yellow oil was obtained after extracting with hexane and washing with water, and it was dried over $CaCl_2$ and the solvent removed. It was purified by bulb-to-bulb distillation at 180 °C/1.5 mbar. (2.88 g, 72% yield). IR (cm^{-1}): 3102, 3081, 1635, 1537, 1518, 1462, 1362, 1236, 1070, 827, 665. ^{1}H NMR (ppm): 7.47 (1H, d, J = 4.9 Hz), 6.97 (1H, d, J = 5.0 Hz), 3.77 (3H, s), 1.53 (6H, m), 1.32 (6H, m), 1.08 (6H, m), 0.88 (9H, t, J = 7.2 Hz). ^{13}C NMR (ppm): δ 164.90, 130.64, 116.02, 111.88, 58.60, 28.94, 27.13, 13.57, 10.53. Anal. Calcd for $C_{17}H_{32}SOSn$: C, 50.66; H, 7.95; S, 7.95. Found: C, 50.71; H, 8.08; S, 7.52.

1,4-Bis(3-methoxy-2-thienyl)benzene (BTBOMe, X = OMe). Into a 25 mL round-bottom flask were placed TTOMe

(2.54 g, 6.30 mmol), 1,4-dibromobenzene (0.71 g, 3.0 mmol), $Pd(PPh_3)_2Cl_2$ (0.042 g, 0.060 mmol) and DMF (6 mL). The mixture was stirred under N_2 for 24 h at 120 °C and then cooled. The solvent and the side product Bu_3SnBr was removed under reduced pressure. The residue was extracted with $CHCl_3$, washed with water, and dried over $CaCl_2$, and $CHCl_3$ was removed. Isolation by silica gel chromatography using hexane−$CHCl_3$ (1:1) as eluant offered the product. (0.61 g, 67% yield, mp 115−116 °C). EIMS *m/z* (relative intensity): 302 (M^+, 100%). HRMS: calculated for $C_{16}H_{14}S_2O_2$ (M^+), 302.0435; found, 302.0415. IR (cm^{-1}): 3088, 3048, 3019, 2934, 2849, 1635, 1553, 1510, 1458, 1433, 1379, 1236, 1066, 858, 831, 648. ^1H NMR (ppm): 7.73 (4H, s), 7.14 (2H, d, J = 5.5 Hz), 6.93 (2H, d, J = 5.5 Hz), 3.92 (6H, s). ^{13}C NMR (ppm): δ 153.75, 131.39, 126.72, 125,34, 121.87, 117.48, 58.67. Anal. Calcd for $C_{16}H_{14}S_2O_2$: C, 63.58; H, 4.64; S, 21.19. Found: C, 62.17; H, 3.47; S, 19.92.

General Procedure for the Preparation of 1,4-Bis(5-bromo-3-X-2-thienyl)benzene (DBBTBX, X = OMe, H, Cl). BTBX (4.13 mmol) was dissolved in a mixture of $CHCl_3$ (30 mL) and AcOH (30 mL) followed by a dropwise addition of bromine (1.33 g, 8.31 mmol) solution. The mixture was stirred at room temperature for 4 h, and the reaction was terminated by filtering and washing with Na_2CO_3 aqueous solution.

1,4-Bis(5-bromo-3-methoxy-2-thienyl)benzene (DBBTBOMe, X = OMe). The residue was isolated by flash chromatography as a yellow solid. (79% yield, mp 153−154 °C). EIMS *m/z* (relative intensity): 462 ($M^+ + 4$, 86), 460 ($M^+ + 2$, 100), 458 (M^+, 80%). HRMS: calculated for $C_{16}H_{12}S_2O_2Br_2$ ($M^+ + 2$), 459.8624; found, 459.8647. IR (cm^{-1}): 3102, 3046, 3015, 2928, 2849, 1653, 1555, 1506, 1458, 1433, 1362, 1203, 1076, 858, 825, 455. ^1H NMR (ppm): 7.61 (4H, s), 6.91 (2H, s), 3.87 (6H, s). ^{13}C NMR (ppm): δ 152.57, 130.80, 126.62, 121.80, 120.72, 109.37, 58.88. Anal. Calcd for $C_{16}H_{12}S_2O_2Br_2$: C, 41.74; H, 2.61; S, 13.91; Br, 34.78. Found: C, 42.36; H, 2.24; S, 12.60; Br 34.50.

1,4-Bis(5-bromo-2-thienyl)benzene (DBBTBH, X = H). The solid was collected, mixed with ethanol, and stirred and the supernatant decanted. The precipitate was then mixed and washed with water, Na_2CO_3 aqueous solution, water, and ethanol in turn. The pale yellow solid was finally collected as the product (1.35 g, 81% yield, mp 249−250 °C). EIMS *m/z* (relative intensity): 402 ($M^+ + 4$, 70), 400 ($M^+ + 2$, 100), 398 (M^+, 62%). HRMS: calculated for $C_{14}H_8S_2Br_2$ ($M^+ + 2$), 399.8414; found, 399.8406. IR (cm^{-1}): 3094, 3043, 3017, 1635, 1541, 1499, 1433, 827, 798, 459. ^1H NMR (ppm): 7.51 (4H, s), 7.07 (2H, d, J = 3.8 Hz), 7.03 (2H, d, J = 3.8 Hz). Anal. Calcd for $C_{14}H_8S_2Br_2$: C, 42.00; H, 2.00; S, 16.00; Br, 40.00. Found: C, 41.96; H, 1.74; S, 15.44; Br, 39.63.

1,4-Bis(5-bromo-3-chloro-2-thienyl)benzene (DBBTBCl, X = Cl). It was recrystallized from $CHCl_3$ to offer a plate form product (92% yield, mp 191−192 °C). EIMS *m/z* (relative intensity): 474 ($M^+ + 8$, 12), 472 ($M^+ + 6$, 64), 470 ($M^+ + 4$, 98), 468 ($M^+ + 2$, 100), 466 (M^+, 62%). HRMS: calculated for $C_{14}H_6S_2Cl_2Br_2$ ($M^+ + 2$), 467.7654; found, 467.7662. IR (cm^{-1}): 3098, 3043, 3019, 1635, 1543, 1497, 1439, 854, 821, 619, 476. ^1H NMR (ppm): 7.66 (4H, s), 6.99 (2H, s). ^{13}C NMR (ppm): δ 137.50, 134.80, 131.61, 128.56, 121.05, 111.07. Anal. Calcd for $C_{14}H_6S_2Cl_2Br_2$: C, 35.82; H, 1.28; S, 13.65; Cl, 15.14; Br, 34.11. Found: C, 35.73; H, 0.78; S, 13.28; Cl, 14.77; Br, 32.77.

1,4-Bis(5-bromo-3-cyano-2-thienyl)benzene (DBBTBCN, X = CN). Into a 25 mL RBF sample were placed BTBCN (0.40 g, 1.4 mmol), AcOH (7 mL), and bromine (0.87 g, 5.4 mmol). The mixture was stirred under reflux overnight at 110 °C and then poured into $CHCl_3$ (200 mL), filtered, and washed by $CHCl_3$, acetone, water, Na_2CO_3 solution, water, and acetone in turn. A yellow solid was finally obtained as the product. (0.51 g, 84% yield, mp > 300 °C). EIMS *m/z* (relative intensity): 452 ($M^+ + 4$, 82), 450 ($M^+ + 2$, 100), 448 (M^+, 80%). HRMS: calculated for $C_{16}H_6S_2N_2Br_2$ ($M^+ + 2$), 449.8318; found, 449.8315. IR (cm^{-1}): 3104, 3044, 3019, 2234,1676, 1593, 1497, 1435, 843, 829, 750, 463. Anal. Calcd for $C_{16}H_6S_2N_2Br_2$: C, 42.67; H, 1.33; S, 14.22; N, 6.22; Br, 35.56. Found: C, 43.00; H, 0.86; S, 14.26; N, 5.31; Br, 35.01.

Synthesis of 1,4-Bis(tributylstannyl)-2,5-dioctylbenzene (DTDOB). 1,4-Dioctylbenzene and 1,4-dibromo-2,5-dioctylbenzene were synthesized from 1,4-dibromobenzene according to the literature.[21]

1,4-Bis(tributylstannyl)-2,5-dioctylbenzene (DTDOB). 2,5-Dibromo-1,4-dioctylbenzene (10.0 g, 21.7 mmol) was dissolved in toluene (72 mL) in a 250 mL round-bottom flask equipped with a condenser under N_2. BuLi (1.1 M in hexane, 39.4 mL, 43.4 mmol) was syringed in. The mixture was refluxed for 8 h and then cooled to 0 °C. After Bu_3SnCl (14.1 g, 43.4 mmol) in toluene (20 mL) was transferred via a cannula, the reaction mixture was heated under reflux for 2 h. Upon being cooled, the mixture was extracted with hexane, washed with water, and dried over $CaCl_2$. Hexane, toluene, and unreacted Bu_3SnCl were removed in turn under reduced pressure. Because of the difficulty in purification, the residue was used as thus obtained. Structural analysis by ^1H NMR, ^{13}C NMR and FTIR spectra show that the titled compound is the main component in the residue, besides the minor contents of 1,4-dioctylbenzene and 1,4-dibromo-2,5-dioctylbenzene. The yield corresponding to the titled compound is 63%. IR (cm^{-1}): 3046, 2957, 2926, 2855, 1597, 1524, 1464, 875, 864, 588. ^1H NMR (ppm): 7.19 (2H, s), 2.48 (4H, t, J = 7.8 Hz), 1.52 (16H, m), 1.32 (32H, m), 1.04 (12H, m), 0.89 (24H, m). ^{13}C NMR (ppm): δ 145.70, 141.25, 136.06, 39.00, 32.51, 31.83, 29.78, 29.57, 29.21, 29.14, 27.36, 22.58, 13.98, 13.53, 10.31.

Synthesis of Polymers. General Procedure for the Stille Coupling Preparation of Poly[1,4-bis(3-X-2,5-thienylene)phenylene-*alt*-2,5-dioctyl-1,4-phenylene] (PBTX, X = OMe, H, Cl, Br, and CN). DBBTBX (1.49 mmol) and DTDOB (1.32 g, 1.50 mmol) were placed into a round-bottom flask containing DMF (10 mL) and $Pd(PPh_3)_2Cl_2$ (0.021 g, 0.030 mmol). The mixture was stirred under N_2 at 110 °C for 48 h and then terminated by cooling to ambient temperature and poured into methanol. Solid polymer was collected after filtering and Soxhlet washing with methanol and acetone overnight, respectively. The soluble fraction was extracted with $CHCl_3$ and then reprecipitated from methanol.

Poly[1,4-bis(3-methoxy-2,5-thienylene)phenylene-*alt*-2,5-dioctyl-1,4-phenylene] (PBTOMe). Yield: 35%. ^1H NMR (ppm): 7.75 (m), 7.15 (m), 7.03 (m), 6.94 (m), 3.98 (m), 2.74 (m), 2.60 (m), 1.55 (m), 1.25 (m), 0.87 (m). ^{13}C NMR (ppm): 153.83, 126.52, 115.59, 113.15, 58.75, 31.79, 29.52, 29.17, 22.58, 14.01. Anal. Calcd for $\{C_{19}H_{24}S_1O_1\}$: C, 76.00; H, 8.00; S, 10.67. Found: C, 67.26; H, 6.05; S, 14.24.

Poly[1,4-bis(2,5-thienylene)phenylene-*alt*-2,5-dioctyl-1,4-phenylene] (PBTH). Yield: 43%. ^1H NMR (ppm): 7.63 (m), 7.34 (m), 7.27 (m), 7.20 (m), 7.11 (m), 7.05 (m), 7.00 (d, J = 3.7), 2.74 (m), 2.60 (m), 1.55 (m), 1.25 (m), 0.87 (m). Anal. Calcd for $\{C_{18}H_{22}S_1\}$: C, 80.00; H, 8.15; S, 11.85. Found: C, 63.90; H, 4.90; S, 19.21.

Poly[1,4-bis(3-chloro-2,5-thienylene)phenylene-*alt*-2,5-dioctyl-1,4-phenylene] (PBTCl). Yield: 37%. ^1H NMR (ppm): 7.77 (m), 7.29 (d, J = 5.4 Hz), 7.19 (m), 7.13 (m), 7.01 (d, J = 5.3 Hz), 6.94 (m), 2.76 (m), 2.58 (m), 1.54 (m), 1.25 (m), 0.87 (m). Anal. Calcd for $\{C_{18}H_{21}S_1Cl_1\}$: C, 70.94; H, 6.90; S, 10.51; Cl, 11.66. Found: C, 61.87; H, 5.06; S, 13.28; Cl, 14.91.

Poly[1,4-bis(3-bromo-2,5-thienylene)phenylene-*alt*-2,5-dioctyl-1,4-phenylene] (PBTBr). Yield: 48%. ^1H NMR (ppm): 7.77 (m), 7.31 (d, J = 5.4 Hz), 7.19 (m), 7.14 (m), 7.07 (d, J = 5.3 Hz), 6.99 (s), 2.74 (m), 2.60 (m), 1.55 (m), 1.25 (m), 0.88 (m). Anal. Calcd for $\{C_{18}H_{21}S_1Br_1\}$: C, 61.89; H, 6.02; S, 9.17; Br, 22.92. Found: C, 60.05; H, 5.51; S, 11.65; Br, 19.20.

Poly[1,4-bis(3-cyano-2,5-thienylene)phenylene-*alt*-2,5-dioctyl-1,4-phenylene] (PBTCN). Yield: 46%. ^1H NMR (ppm): 7.94 (m), 7.44 (m), 7.42 (d, J = 5.3 Hz), 7.34 (d, J = 5.3 Hz), 7.20 (m), 2.74 (m), 2.60 (m), 1.55 (m), 1.25 (m), 0.87 (m). Anal. Calcd for $\{C_{19}H_{21}S_1N_1\}$: C, 77.29; H, 7.12; S, 10.85. Found: C, 69.01; H, 5.93; S, 12.99.

Synthesis and Structure Characterization. The main compounds used in the polymer synthesis are 1,4-bis(3-X-2-thienyl)benzene, BTBX (X = OMe, H, Cl, Br, CN). Their dibrominated compounds, 1,4-bis(5-bromo-3-X-2-thienyl)benzene DBBTBX (X = OMe, H, Cl, Br, CN), were directly

Scheme 1[a]

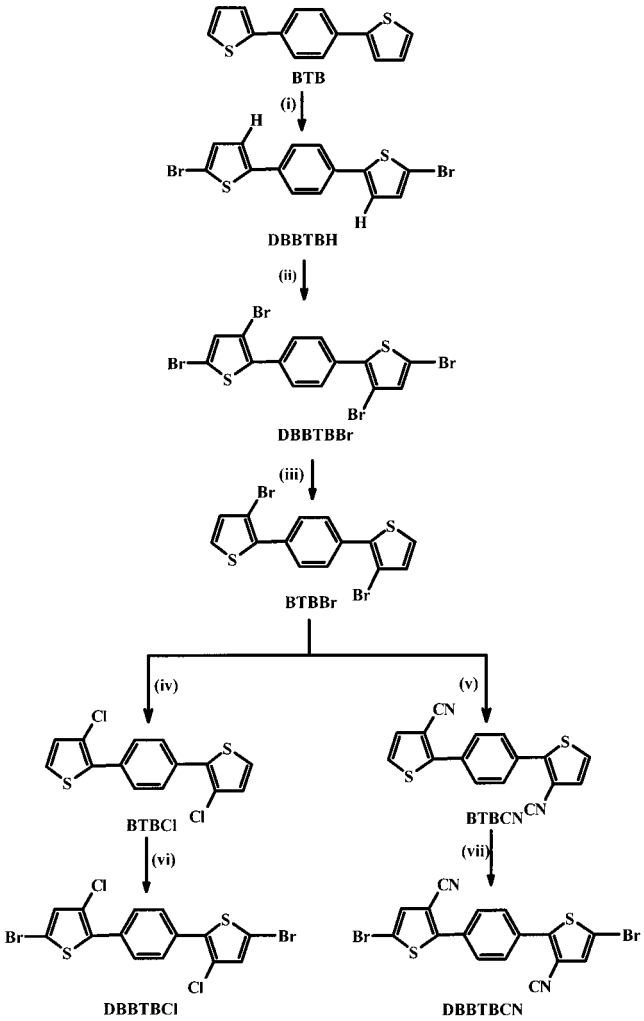

[a] Reagents and conditions: (i), ii, and vi) 2 equiv of bromine, AcOH/$CHCl_3$; (iii) zinc dust, 2-propanol; (iv) CuCl, DMF; (v) CuCN, DMF; (vii) bromine, AcOH.

Scheme 2[a]

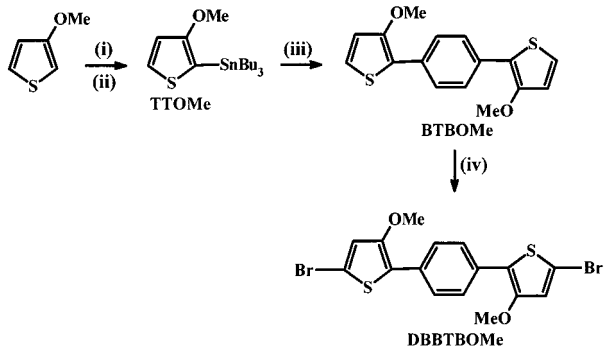

[a] Reagents and conditions: (i) BuLi, Et_2O; (ii) Bu_3SnCl, Et_2O; (iii) 1,4-dibromobenzene, $Pd(PPh_3)_2Cl_2$, DMF; (iv) 2 equiv of bromine, AcOH/$CHCl_3$.

employed in the synthesis of PBTX polymers. DBBTBX (X = H, Cl, Br, CN) were synthesized in the ways shown in Scheme 1, which are relevant to each other. DBBTBOMe, on the other hand, was produced in a different way as depicted in Scheme 2.

Synthesis of 1,4-Bis(5-bromo-3-X-2-thienyl)benzene, DBBTBX (X = H, Cl, Br, CN). The successful synthesis of $BTBSC_n$ in another report[19] encourages us to synthesize the current monomers in a similar fashion. Scheme 1 shows the synthetic routes to 1,4-bis(5-bromo-2-thienyl)benzene (DBBTBH, X = H), 1,4-bis(3,5-dibromo-2-thienyl)benzene (DBBTBBr, X = Br), 1,4-bis(3-chloro-2-thienyl)benzene (BTBCl), 1,4-bis(3-cyano-2-thienyl)benzene (BTBCN) and from the latter two, 1,4-bis(5-bromo-3-chloro-2-thienyl)benzene (DBBTBCl, X = Cl) and 1,4-bis(5-bromo-3-cyano-2-thienyl)benzene (DBBTBCN, X = CN).

Their structures are mainly verified by MS, NMR (BTBCN and DBBTBH are only slightly soluble and the solubility is insufficient for a ^{13}C NMR spectrum to be detected. Accordingly, only ^1H NMR spectra were obtained for them.) and FTIR spectra. For example, the $C_\phi-H$, $C_\alpha-H$, and $C_\beta-H$ resonances of BTBCl are exhibited at δ 7.74, 7.28, and 7.01 ppm, respectively, in its ^1H NMR spectrum, while those of BTBCN are displayed at δ 7.89, 7.39, and 7.32 ppm, respectively. DBBTBCN is insoluble. Its formation is confirmed by mass spectra and the existence of C≡N stretching at 2234 cm^{-1},[22] $C_\beta-H$ out-of-plane bending at 829 cm^{-1}, and the para-substitution pattern of the phenylene unit at 843 cm^{-1} in its FTIR spectrum. The presence of bromine is supported by the microanalysis result.

Synthesis of 1,4-Bis(5-bromo-3-methoxy-2-thienyl)benzene (DBBTBOMe). The synthetic route to 1,4-bis(3-methoxy-2-thienyl)benzene (BTBOMe) and its dibrominated compound, DBBTBOMe, is shown in Scheme 2. 3-Methoxythiophene was lithiated followed by conversion to organotin compound, 2-tributylstannyl-3-methoxythiophene (TTOMe). Stille coupling between TTOMe and 1,4-dibromobenzene led to BTBOMe. Bromination of the latter offered DBBTBOMe.

Synthesis of 1,4-Bis(tributylstannyl)-2,5-dioctylbenzene (DTDOB). The synthetic route to 1,4-bis(tributylstannyl)-2,5-dioctylbenzene (DTDOB) is shown in Scheme 3. 1,4-Dibromobenzene was converted to 1,4-dibromo-2,5-dioctylbenzene according to the literature.[21] The latter was lithiated[23] and then converted to DTDOB. The ^1H NMR spectrum of DTDOB shows one singlet at δ 7.19 ppm ascribed to the $C_\phi-H$ resonance and a few sets of resonances at δ 2.48, 1.52, 1.32, 1.04, and 0.89 ppm in the aliphatic range, due to the resonance overlapping of protons on the octyl and tributylstannyl groups.

Synthesis of Polymers. As shown in Scheme 3, Stille coupling between the two starting materials DBBTBX and DTDOB, at elevated temperatures (>110 °C), afforded the polymers PBTX (X = OMe, H, Cl, Br, CN).

^1H MNR spectroscopy was employed to monitor and verify the formation of each polymer during synthesis using DBBTBX as references. The occurrence of coupling between thienylene and phenylene rings is manifested by the appearance of broad resonances of internal $C_\beta-H$ on thienylene ring at δ 6.94 (PBTOMe), 7.11 (PBTH), 7.13 (PBTCl), 7.14 (PBTBr), and 7.44 (PBTCN) ppm. Except for PBTOMe, whose terminal aromatic rings are mainly phenylene moieties as indicated by the very low intensity of $C_\alpha-H$ resonances in ^1H NMR spectrum, all the other polymers are mainly capped by thienylene rings under such a reaction condition. The molecular weights of the soluble parts are not high as indicated by the presence of $C_\alpha-H$ and $C_\beta-H$ resonances associating with the terminal rings. The number of aromatic rings in a polymer (PBTX, X = H, Cl, Br, and CN) chain, evaluated from the integrals of the $C_\beta-H$ resonances on both the internal and end thienylene rings, is almost the same as that from GPC (next section).

The polymer structures are also verified by the FTIR spectroscopy. The accomplishment of coupling between α-site of thienylene ring and phenylene unit was indicated by the strong $C_\beta-H$ out-of-plane bending at around 830 cm^{-1}, the weak $C_\alpha-H$ stretching at around 3080 cm^{-1}, the existences of $C_\beta-H$ stretching at around 3040 cm^{-1}, and the $C_\phi-H$ stretching at 3020 cm^{-1}. The 1,2,4,5-tetrasubstitution and 1,4-disubstitution patterns of phenylene rings are found at ca. 860−900 and 800−860 cm^{-1} [24] for the $C_\phi-H$ out-of-plane bending modes, respectively. In addition, the characteristic vibration of each functional group is indicated at 2224 cm^{-1} (C≡N for PBTCN), 611 cm^{-1} ($C_\beta-Br$ for PBTBr), 619 cm^{-1} ($C_\beta-Cl$ for PBTCl), 794 cm^{-1} ($C_\beta-H$ for PBTH) or 1074, 1202, and 1261 cm^{-1} (C−O−C symmetric and unsymmetric stretchings for PBTOMe). The existences of octyl side chain and

Scheme 3[a]

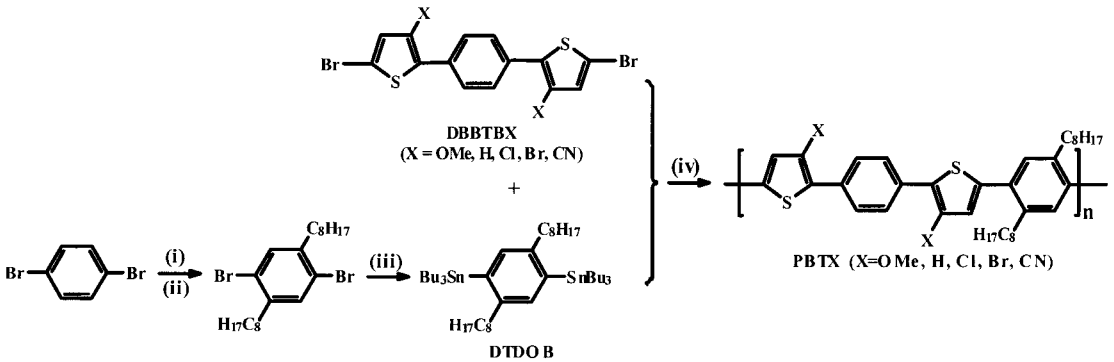

[a] Reagents and conditions: (i) $C_8H_{17}MgBr$, Et_2O; (ii) Br_2; (iii) (a) BuLi, Et_2O; (b) Bu_3SnCl, Et_2O; (iv) $Pd(PPh_3)_2Cl_2$, DMF−toluene.

Table 1. Summary of Number-Averaged Molecular Weights (M_n), Polydispersity Indices (PDI), and Conductivities (σ)

	GPC results		σ[a] (S cm^{-1})	
polymer	M_n	PDI	I_2-doped	$FeCl_3$-doped
PBTOMe	2150	1.2	1.4×10^{-1}	9.2×10^{-3}
PBTH	1800	1.1	*b*	4.2×10^{0}
PBTCl	2000	1.1	3.8×10^{-3}	2.0×10^{-6}
PBTBr	2700	1.4	*b*	*b*
PBTCN	2100	1.2	*c*	*c*

[a] The insoluble parts of the polymers are employed in the conductivity measurements as the soluble parts are insufficient. [b] Pellets are too brittle to be measured. [c] PBTCN cannot be doped by I_2 or $FeCl_3$.

thienylene and phenylene rings are evidenced by the stretchings at around 2924, 1458, and 1600 cm^{-1}.

Results and Discussion

Physical Properties. PBTOMe is a dark red powder while the others are either brown or orange. The polymers are only partially soluble in $CHCl_3$, THF, toluene, and xylene. In addition, PBTOMe is partially soluble in polar solvents, such as CH_3CN and CH_3NO_2. The soluble fraction was extracted with $CHCl_3$ and then reprecipitated from methanol. This fraction of the polymer was used for GPC and spectral measurements as well as film casting.

As shown in Table 1, the number-averaged molecular weights (M_n) of the soluble fraction as determined by GPC are in the range of 1800−2700 and the polydispersity indices (PDI) are in the range of 1.1−1.4. The molecular weights correspond to 12−16 aromatic rings in the polymer chains. As the GPC determination involves only the soluble fraction, the insoluble part should have a higher molecular weight and hence a longer polymer chain. This fraction of the polymer is used for conductivity measurement as the soluble part is insufficient.

The color of the polymers changes to black when doped with I_2 or $FeCl_3$ except for PBTCN, which shows a slight color change from brown to a darker shade which faded quickly back to the original color in air. The pellet of I_2- or $FeCl_3$-doped PBTBr is too brittle for the conductivities to be measured, but that of PBTCl is not. Thick films of electrochemically generated poly(3-bromothiophene)[25] and poly(3,3′-dibromo-2,2′-bithiophene)[26] were reported to show similar fracture brittleness. The $FeCl_3$-doped PBTH has the highest conductivity (4.2 S cm^{-1}) of all the polymers reported in this paper and earlier reports,[15−19] but when I_2 was employed as a dopant, the inside of the pellet was not properly doped as revealed by the retention of the color of the neutral form. The electron-donating group functionalized polymer, PBTOMe, shows moderate conductivity in both I_2- and $FeCl_3$-doped states.

Table 2. Absorption Peak Wavelengths (λ_{max}) and Emission Peak Wavelengths (λ_{em}), Solution Quantum Yields, Stokes Shifts, and Band Gaps for PBTX Polymers in Solution and as Solid Film

sample	λ_{max} (nm)[a]	λ_{em} (nm)[a]	Stokes shift (nm)[b]	quantum yield (%)[c]	band gap (eV)[d]
		Solution			
PBTOMe	316, 382, *446*	536	90	25	
PBTH	406	*476*, 506	70	94	
PBTCl	384	478	94	77	
PBTBr	382	488	106	40	
PBTCN	384	480	96	60	
		Film			
PBTOMe	*452*, 470, 509	540	31		2.03
PBTH	*394*, 437, 470	*467*−483	−3		2.44
PBTCl	400	470, *492*, 510	70		2.56
PBTBr	401	470, *484*, 507	69		2.53
PBTCN	388	532	144		2.44

[a] Some of the samples exhibit shoulders in absorption and emission spectra. The italicized values are the maxima. [b] Stokes shift is the wavelength difference of (0 → 0) peaks in emission and absorption spectra.[30] [c] Relative to quinine sulfate in 0.1 M H_2SO_4. [d] Evaluated from optical band edges.

UV−Vis Absorption and Fluorescence Spectra. Table 2 summarizes the absorption peak wavelengths (λ_{max}) and emission peak wavelengths (λ_{em}) of the polymers in $CHCl_3$ solution and as solid films, together with their solution quantum yields, the optical band gaps (E_g, evaluated from the band edges. In the case of absorption with shoulders, E_g is evaluated from the optical band edge of 0 → 0 shoulder.) and Stokes shifts. It can be seen that in the solution phase, substitution with electron-donating group, OMe, shifts both the λ_{max} and λ_{em} bathochromically, in comparison with PBTH. On the other hand, electron-withdrawing groups shift the λ_{max} of the corresponding polymers blue-ward although the amount of shift is almost the same for CN, Br, and Cl. In addition, the absorption spectrum of PBTOMe and emission spectrum of PBTH show fine structures in solution, which are usually assigned to the vibronic broadening.[27] The quantum yields relative to quinine sulfate range from 25 to 94%, of which the lowest one is PBTOMe. PBTH shows a higher quantum yield than those polymers substituted by electron-

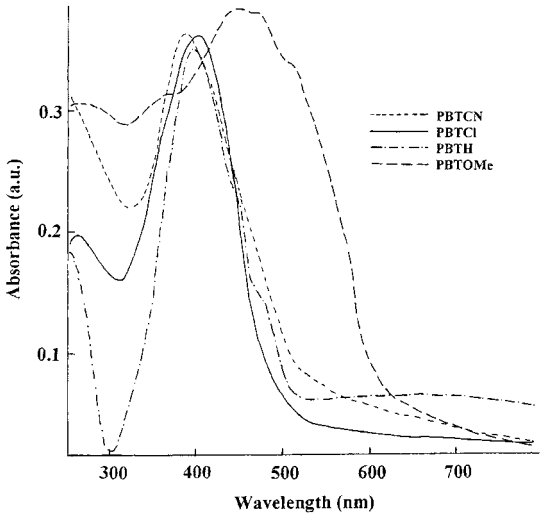

Figure 1. UV−vis absorption spectra of PBTX films. The spectrum of PBTBr is almost the same as that of PBTCl and is, therefore, not shown.

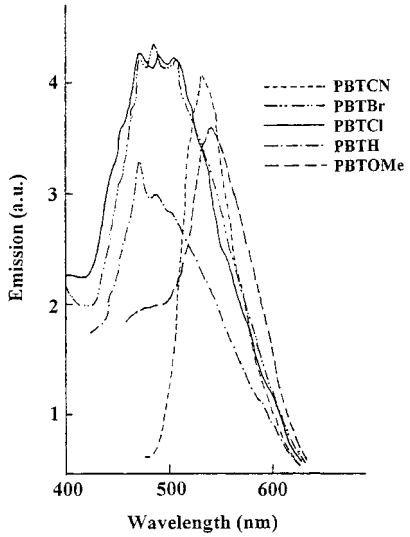

Figure 2. Emission spectra of PBTX films.

donating or -withdrawing groups. Among the polymers substituted by electron-withdrawing groups, the quantum yield of PBTBr is lower than that of PBTCl. For the halogen-substituted polymers, the lowering in quantum yield in comparison with PBTH is ascribed to the intersystem crossing (ISC) effects. This effect is more pronounced for bromine than chlorine.[28] The lower quantum yield of PBTBr and PBTCl may also be attributed to the strong steric hindrance between the substituents, which gives rise to a less planar structure in PBTCl and PBTBr than in PBTH.

The absorption and emission spectra of the polymer films are shown in Figures 1 and 2, respectively. In absorption spectra, PBTOMe and PBTH show two shoulder peaks due to vibronic transitions. Some researchers, however, have assigned the shoulder peaks to polymer molecules possessing different conjugation lengths.[29] The appearance of vibronic bands was associated with the structure ordering resulting from substituent interactions.[27] The bathochromic shift of absorption peaks in going from solution to film for both PBTOMe and PBTH (Table 2), is indicative of an ordering process from solution to film. The small Stokes shifts [wavelength differences between (0 → 0) peaks in emission and absorption spectra[30]] found for PBTOMe and PBTH films, suggest one possibility that the structures in the ground state for both the polymers are already quite coplanar, as compared to their excited states.[30,31] On the other hand, PBTCl and PBTBr exhibit large Stokes shifts. The very large Stokes shift (144 nm) in PBTCN may be due to the stable and planar configuration of its excited state and thus favor a radiative transition of interchain excited state, as in the case of CN−PPV.[32]

The optical band gap of PBTOMe is narrowed by 0.41 eV in comparison with PBTH, while those of PBTCl and PBTBr are widened slightly. However, the E_g of PBTCN is the same as that of PBTH. This situation was also found in the cyano-substituted PPV[9] and was attributed to an overall stabilization of the backbone frontier electronic levels by the electron-withdrawing nature of CN group.[33]

Cyclic Voltammetry. The substitution with electron-withdrawing or -donating groups has exerted a rather strong effect on the polymers' electronic structures, as supported by their spectral behaviors. Cyclic voltammetry (CV) provides even more detailed information about the electronic structures of electroactive polymers, such as IP, EA and band gap,[34] as discussed earlier.[18,19] The PBTX series of polymers was investigated by CV in the same 1 M acetonitrile solution of Bu_4NBF_4 used previously.[18,19] Their CV curves are presented in Figure 3. PBTH, PBTCl, PBTBr, and PBTOMe show concurrent p- and n-doping accompanied by sharp color changes, but they are not very stable and the current density decreases upon repeated scanning. The neutral form of PBTOMe is partially soluble in CH_3CN, and its solubility is enhanced in the doped states, especially in the n-doped one. Its solubility and instability may be responsible for the lack of dedoping peaks. The CV plot of PBTCl is similar to that of PBTBr, but PBTH shows the most stable p- and n-doping states relative to other polymers. For PBTCN, it is only n-dopable as its anodic scanning did not show any color change accompanying the emergence of an ill-defined anodic peak. This is consistent with the unsuccessful chemical doping of PBTCN after being oxidized by I_2 or $FeCl_3$. Table 3 lists the onset potentials of p- and n-doping processes and the deduced ionization potentials (IP), electron affinities (EA), and electrochemical band gaps (E_g, evaluated from the onset potential differences of p- and n-doping processes). The data show that the introducing of electron-donating methoxy group to the polymer backbone lowers the onset oxidation potential and therefore, IP. However, its EA is increased to a greater extent, resulting in a significant decrease in the band gap (by 0.48 eV), in comparison with PBTH. The electron-withdrawing groups, chlorine and bromine, have similar influence on the electronic structure. They raise the IP and lower the EA slightly and as an overall result, the band gap is slightly increased. For PBTCN, the strong electron-withdrawing ability of the cyano group raises the IP to so high a level that it cannot be detected electrochemically before the polymer degraded. Reduction of PBTCN is easy, as shown in Figure 3. The resulting electron affinity is 0.51 eV higher than that of PBTH. Although the electrochemical band gap cannot be deduced because of the lack of onset oxidation potential, its optical band gap is the same as that of PBTH. If the electrochemical band gap of PBTCN is assumed to be the same as that of PBTH, the onset

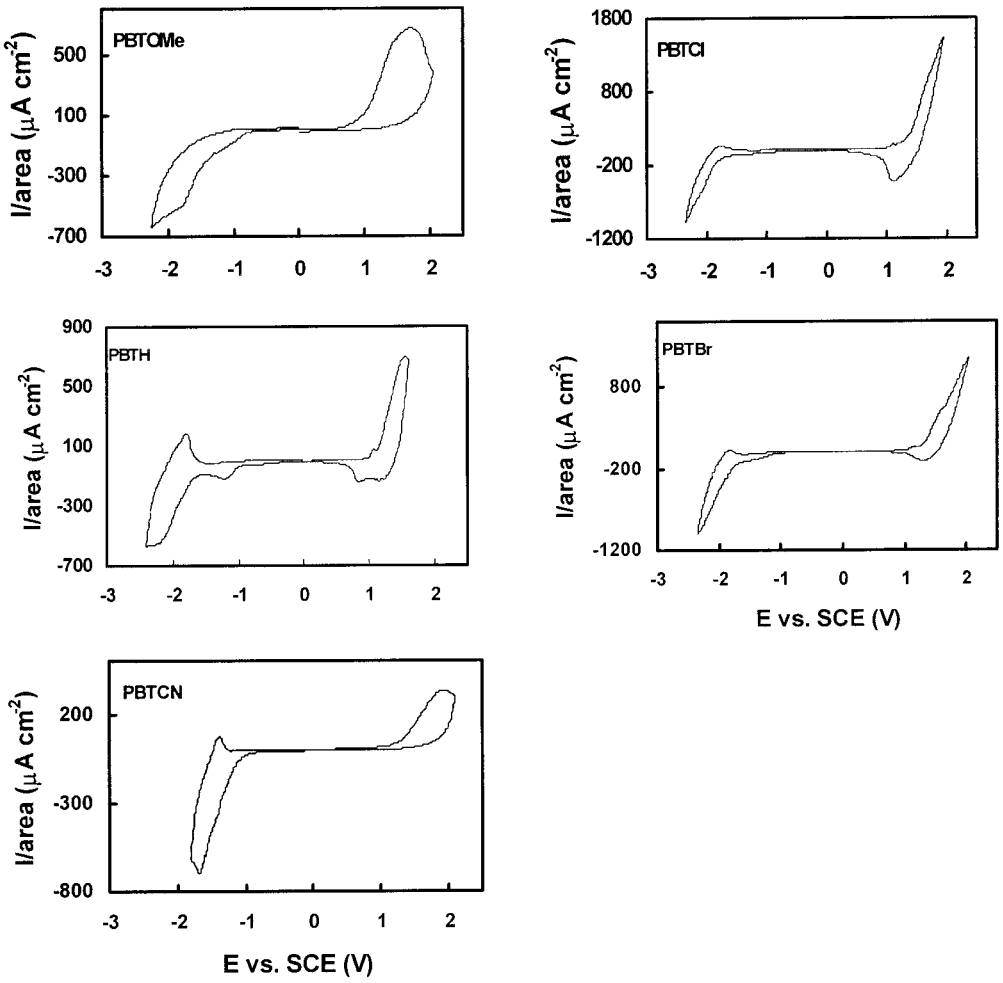

Figure 3. CV plots for PBTX polymers.

Table 3. Summary of Electrochemical Results from CV

	p-doping		n-doping		
polymer	E_{on} (V)	IP (eV)	E_{on} (V)	EA (eV)	band gap (eV)[b]
PBTOMe	0.96	5.46	−1.28	3.22	2.24
PBTH	1.10	5.60	−1.62	2.88	2.72
PBTCl	1.24	5.74	−1.66	2.84	2.90
PBTBr	1.26	6.76	−1.64	2.86	2.90
PBTCN	1.61[a]	6.11[a]	−1.11	3.39	2.72[a]

[a] The values are predicted based on the assumption that the electrochemical band gap of PBTCN is the same as that of PBTH because their optical band gaps are the same. [b] Electrochemical band gaps.

oxidation potential and correspondingly, the IP, are predicted for PBTCN as shown in Table 3.

Bredas and Heeger[33] had calculated the influence of methoxy and cyano groups on the electronic structures of PPV derivatives. Their results show that substitution with methoxy moieties lowers the band gaps mainly through reducing IP and EA but the influence on IP is greater. Our observation with PBTOMe is different from this calculation, as the EA of PBTOMe is raised instead of reduced. This is consistent with the observation obtained in SR-functionalized polymers.[19] However, the electronic effect of CN group on the polymer is in good agreement with their calculation: both IP and EA of PBTCN are increased, but the E_g remained almost unchanged.

The n-doping onset potential of PBTCN is more anodic than that of CN−PPV (E_{on} of n-doping is −1.6 V vs Ag/Ag^+ or −1.36 V vs SCE), while its p-doping onset potential is too high to be detected by CV. This indicates that PBTCN has a better electron injection and transport property and at the same time, is a better hole blocking material than CN−PPV (E_{on} of p-doping is +0.9 V vs Ag/Ag^+, or +1.14 V vs SCE).[9] The result suggests that it might be an ideal candidate for the use as electron injection and transport layers (ETL), as an efficient electron injection may be realized in devices using stable metals, such as Al, as cathodes. PBTOMe shows comparable EA as CN−PPV but has a quite low IP, suggesting a balanced electron and hole injection might be achieved if it is used as an emission layer, despite its relatively low quantum yield. The p-dopability of the polymers was verified by the change in UV−vis−NIR spectroscopy under applied potentials. Figure 4a shows the spectral change for PBTH in the p-doping process. Two new potential-dependent peaks come out at about 1050 (1.18 eV) and 550 nm (2.25 eV), respectively, corresponding to the transitions from valence band to the two bipolaronic intragap states formed during doping. Their intensities increase with the increase of applied potentials, while that of the $\pi-\pi^*$ transition decreases. However, degradation takes place at potentials higher than +1.8 V. Figure 4b shows the band structure diagram at +1.8 V (the energy gaps are calculated based on absorption peak wavelengths). The transition energies from valence band to the bonding and antibonding bipolaron states are 1.18 eV ($h\nu_1$) and 2.25 eV ($h\nu_2$), respectively, suggesting a symmetric

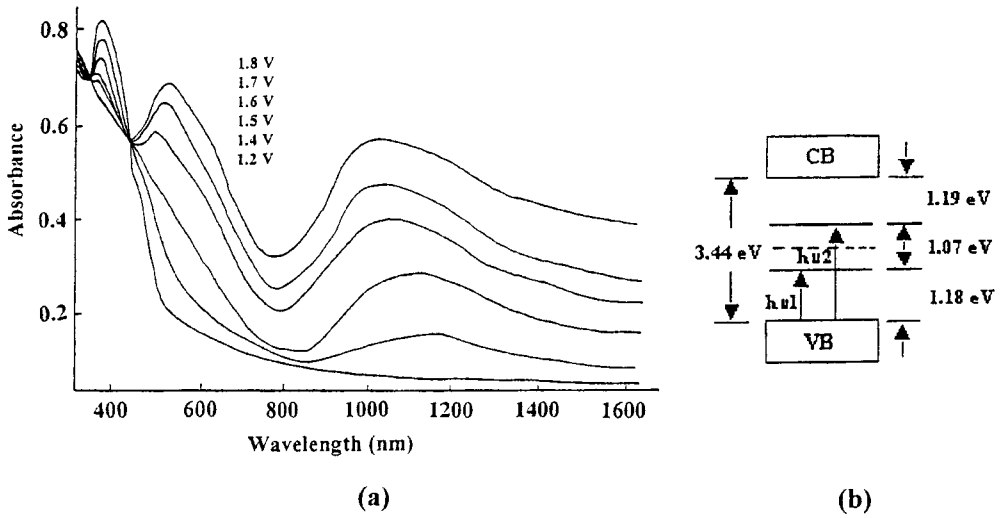

Figure 4. (a) In situ potential-dependent UV−vis−NIR spectra of PBTH during p-doping; (b) Band structure at +1.8 V.

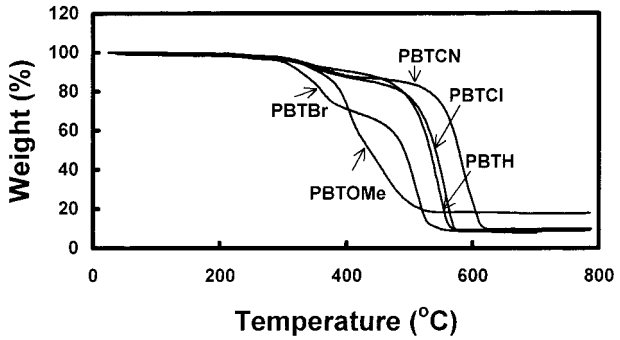

Figure 5. TG plots of PBTX polymers in air.

distribution pattern of the two levels within the $\pi-\pi^*$ gap.

Thermogravimetry of Neutral Polymers. Thermogravimetry (TG) of the PBTX polymers in air atmosphere was carried out, and the thermograms are shown in Figure 5. The onset decomposition temperatures for the major weight loss steps of the PBTX polymers increase as follows: PBTBr < PBTOMe < PBTH ≅ PBTCl < PBTCN. The bromine-substituted PPV derivative was reported to eliminate hydrogen bromine at 180 °C in DSC scanning, indicating a low thermal stability of the bromine derivative.[35] Similar behavior may occur in our polymer system at temperatures higher than 280 °C, resulting in the least thermal stability of PBTBr. As the C−O linkage is easy to break down, the thermal stability of PBTOMe is also low. The thermal stability of PBTH is similar to that of $PBTC_8$,[18] suggesting that the change of distribution pattern of the octyl group on the polymer backbone does not affect the thermal stability very much. In the case of PBTCN, it shows the highest thermal stability among all the five polymers. The strong interchain interaction between cyano groups which leads to strong secondary force and the possible cross-linking between the PBTCN polymer chains may account for the superior thermal stability.

XPS. Similar to polymers previously studied by XPS,[18,19] doping by $FeCl_3$ introduced a new S(2p) environment at a higher bind energy than the neutral sulfur component for PBTX (X = OMe, H, Cl, Br) polymers (not shown), ascribable to the presence of an oxidized sulfur species.[36]

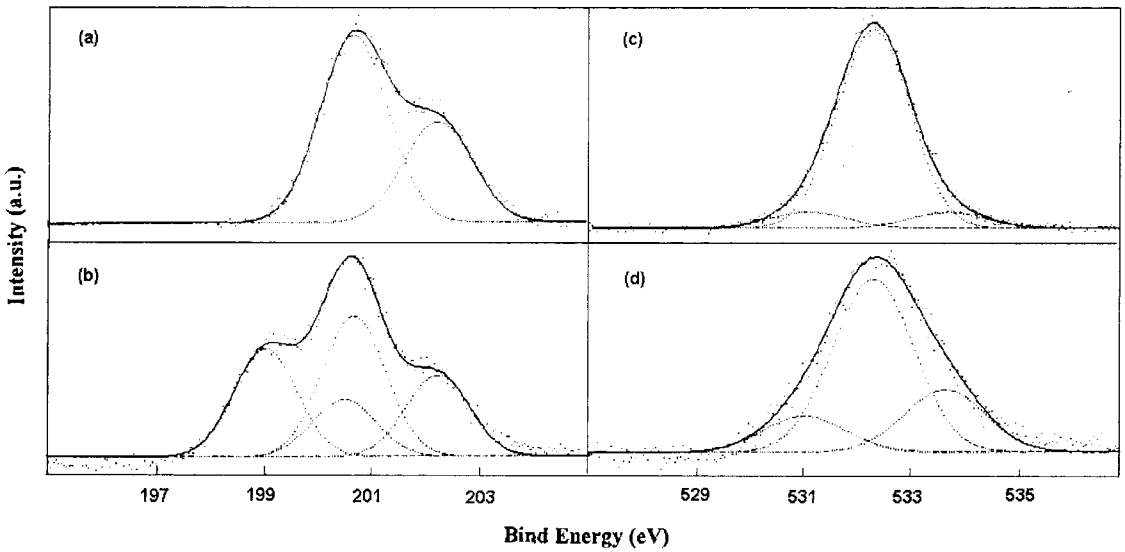

Figure 6. XPS spectra of (a) Cl(2p) of neutral PBTCl, (b) Cl(2p) of $FeCl_3$-doped PBTCl, (c) O(1s) of neutral PBTOMe, and (d) O(1s) of $FeCl_3$-doped BPTOMe.

Table 4. Summary of Figures about Doping Level from XPS

polymer[a]	$[S^+]/[S]$ (%)[b]	$[Cl-Cl_c]_4/[S]$ (%)[c]
PBTOMe	26	60
PBTH	30	43
PBTH-e	20	$[F]_4/[S] = 32$
PBTCl	20	30
PBTBr	23	23

[a] Polymers are all doped by $FeCl_3$, except PBTH-e which is electrochemically doped by BF_4^-. PBTCN cannot be doped by I_2 and $FeCl_3$ or by electrochemical methods, and therefore it is not shown. [b] The value of $[S^+]/[S]$ indicates the amount of positively charged sulfur species as a percentage of total sulfur. Hence, twice the value affords the average number of dopants associated with one monomeric repeating unit, as the latter contains two sulfur atoms. [c] The value of $[Cl-Cl_c]_4/[S]$ indicates the normalized amount (in percentage) of charged chlorine species (Cl^-) corresponding to the total sulfur. Hence, twice the value affords the average number of dopants associated with one monomeric repeating unit, as the latter contains two sulfur atoms.

The Cl(2p) core-level spectra of PBTCl in neutral and $FeCl_3$-doped states are shown in Figure 6, parts a and b, respectively. The doublet at 200.3 and 201.8 eV for the neutral polymer is assigned to the spin−orbit splitting [Cl($2p_{3/2}$) and Cl($2p_{1/2}$)] components of the chlorine species involved in the C−Cl bond (denoted as Cl_c) and is consistent with the literature report.[37] The area ratio of the Cl(2p) core level spectrum to that of sulfur is 1.1:1 (expected 1:1). After doping, two doublets with their Cl($2p_{3/2}$) components lying at 198.6 and 200.3 eV are deconvoluted. The area ratio of the latter doublet to that of sulfur changes to 1.7:1, indicating a concentration increase of C−Cl species due to the chlorination of polymer backbone.[36] The former doublet with Cl($2p_{3/2}$) located at 198.6 eV is usually assigned to the chlorine species involved in the $FeCl_4^-$ species.

O(1s) spectra of PBTOMe in the neutral and $FeCl_3$-doped states are shown in Figure 6, parts c and d, respectively. The O(1s) spectrum of the neutral polymer exhibits a main peak at 532.2 eV due to C−O species as well as two weak components at 531.0 and 533.6 eV respectively, contributed by C═O and H_2O species, respectively. Oxidation of the polymer by $FeCl_3$ causes an overall broadening of the spectrum line shape, due to the intensity increase of the peaks at 531.0 and 533.6 eV, especially the latter. The greatly enhanced peak at 533.6 eV may have partially come from a new species, i.e., the positively polarized oxygen species due to oxidation by the dopant. This species may be formed by the resonance structure of the quinoid configuration of the oxidized polymer, similar to the polymers reported earlier[19] and SR- and OR-substituted polythiophenes reported in the literature.[38,39] The degree of doping evaluated based on XPS results is shown in Table 4. The result for doping level from $[Cl-Cl_c]_4/[S]$ is usually higher than that from $[S^+]/[S]$, as discussed earlier.[18,19] In this context, the latter may provide a more accurate measure of the doping level, as chlorine may exist in other forms.[40] Nevertheless, the very high value of $[Cl-Cl_c]_4/[S]$ obtained for PBTOMe, as compared to $[S^+]/[S]$, supports the doping at both the S and O moieties. This high doping level, however, does not make PBTOMe the most conducting. The partial localization effect of charge carriers on the pendant O atoms gives rise to moderate conductivity (Table 1), as the mobility of charge carriers is greatly reduced, similar to the case of SR-functionalized polythiophenes.[38]

Acknowledgment. Financial support from the National University of Singapore (NUS) under Research Grant RP960613 is gratefully acknowledged. J.M.X. is grateful to the NUS for the award of a research scholarship.

References and Notes

(1) Burroughes, J. H.; Bradley, D. D. C.; Brown, A. R.; Marks, R. N.; Mackay, K.; Friend, R. H.; Burn, P. L.; Holmes, A. B. *Nature* **1990**, *347*, 539.
(2) Braun, D.; Heeger, A. J. *Appl. Phys. Lett.* **1991**, *58*, 1982.
(3) Grem, G.; Leditzky, G.; Ullrich, B.; Leising, G. *Adv. Mater.* **1992**, *4*, 36.
(4) Yang, Y.; Pei, Q.; Heeger, A. J. *J. Appl. Phys.* **1996**, *79*, 934.
(5) Ohmori, Y.; Uchida, M.; Muro, K.; Yoshino, K. *Jpn. J. Appl. Phys.* **1991**, *30*, L1938.
(6) Pomerantz, M.; Cheng, Y.; Kasim, R. K.; Elsenbaumer, R. L. *Synth. Met.* **1997**, *85*, 1235.
(7) Friend, R. H.; Greenham, N. C. In *Handbook of Conducting Polymer*, 2nd ed.; Skotheim, T. A., Elsenbaumer, R. L., Reynolds, J. R., Eds.; Marcel Dekker Inc.: New York, Basel, Switzerland, and Hong Kong, 1998; p 857.
(8) Leising, G.; Tasch, S.; Graupner, W. In *Handbook of Conducting Polymer*, 2nd ed.; Skotheim, T. A., Elsenbaumer, R. L., Reynolds, J. R., Eds.; Marcel Dekker Inc.: New York, Basel, Switzerland, and Hong Kong, 1998; p 868.
(9) Li, X.-C.; Kraft, A.; Cervini, R.; Spencer, G. C. W.; Cacialli, F.; Friend, R. H.; Gruner, J.; Holmes, A. B.; DeMello, J. C.; Moratti, S. C. *Mater. Res. Soc. Symp. Proc.* **1996**, *413*, 13.
(10) Parker, I. D. *J. Appl. Phys.* **1994**, *75*, 1656.
(11) Lux, A.; Holmes, A. B.; Cervini, R.; Davies, J. E.; Moratti, S. C.; Gruner, J.; Cacialli, F.; Friend, R. H. *Synth. Met.* **1997**, *84*, 293.
(12) Grimsdale, A. C.; Cacialli, F.; Gruner, J.; Li, X.-C.; Holmes, A. B.; Moratti, S. C.; Friend, R. H.*Synth. Met.* **1996**, *76*, 165.
(13) Gurge, R. M.; Sarker, A.; Lahti, P. M.; Hu, B.; Karasz, F. E. *Macromolecules* **1996**, *29*, 4287.
(14) Lux, A.; Moratti, S. C.; Li, X.-C.; Grimsdale, A. C.; Davies, J. E.; Raithby, P. R.; Gruner, J.; Cacialli, F.; Friend, R. H.; Holmes, A. B. *Polym. Prepr.* **1996**, *37*, 202.
(15) Ng, S. C.; Xu, J. M.; Chan, H. S. O. *Synth. Met.* **1998**, *92*, 33.
(16) Ng, S. C.; Xu, J. M.; Chan, H. S. O. *J. Mater. Chem.* **1999**, *9*, 381.
(17) Ng, S. C.; Xu, J. M.; Chan, H. S. O. *Synth. Met.* **2000**, *110*, 31.
(18) Ng, S. C.; Xu, J. M.; Chan, H. S. O. *Macromolecules* **2000**, *33*, 7349.
(19) Xu, J. M.; Ng, S. C.; Chan, H. S. O. *Chem. Mater.* Submitted for publication.
(20) Heck, R. F. *Palladium Reagents in Organic Synthesis*; Academic Press: New York, 1985; pp 1−18.
(21) Rehahn, M.; Schluter, A.-D.; Feast, W. J. *Synthesis* **1988**, 386.
(22) Furniss, B. S.; Hannaford, A. J.; Smith, P. W. G.; Tatchell, A. R. *Vogel's Textbook of Practical Organic Chemistry*, 5th ed.; Longman Scientific & Technical: New York, 1989; p 314.
(23) Tanigaki, N.; Masuda, H.; Kaeriyama, K. *Polymer* **1997**, *38*, 1221.
(24) Furniss, B. S.; Hannaford, A. J.; Smith, P. W. G.; Tatchell, A. R. *Vogel's Textbook of Practical Organic Chemistry*, 5th ed.; Longman Scientific & Technical: New York, 1989; p 280.
(25) Kassmi, A. E.; Fache, F.; Lemaire, M. *J. Electroanal. Chem.* **1994**, *373*, 241.
(26) Chan, H. S. O.; Ng, S.-C.; Seow, S.-H.; Moderscheim, M. J. G. *J. Mater. Chem.* **1992**, *2*, 1135.
(27) Roncali, J.; Youssoufi, H. K.; Garreau, R.; Garnier, F.; Lemaire, M. *J. Chem. Soc., Chem. Commun.* **1990**, 414.
(28) Cowan, D. O.; Drisko, R. L. *Elements of Organic Photochemistry*; Plenum Press: New York, London, 1978; p 255.
(29) McCullough, R. D.; Lowe, R. D.; Jayaraman, M.; Anderson, D. L. *J. Org. Chem.* **1993**, *58*, 904.
(30) Bredas, J. L.; Cornil, K.; Meyers, F.; Beljonne, D. In *Handbook of Conducting Polymer*, 2nd ed.; Skotheim, T. A., Elsenbaumer, R. L., Reynolds, J. R., Eds.; Marcel Dekker Inc.: New York, Basel, Switzerland, and Hong Kong, 1998; p 13.
(31) Beljonne, D.; Shuai, Z.; Friend, R. H.; Bredas, J. L. *J. Chem. Phys.* **1995**, *102*, 2042.
(32) Friend, R. H.; Greenham, N. C. In *Handbook of Conducting Polymer*, 2nd ed.; Skotheim, T. A., Elsenbaumer, R. L., Reynolds, J. R., Eds.; Marcel Dekker Inc.: New York, Basel, Switzerland, and Hong Kong, 1998; p 836.

(33) Bredas, J. L.; Heeger, A. J. *Chem. Phys. Lett.* **1994**, *217*, 507.
(34) Pfluger, P.; Street, G. B. *J. Chem. Phys.* **1984**, *80*, 544.
(35) Sarnecki, G. J.; Friend, R. H.; Holmes, A. B.; Moratti, S. C. *Synth. Met.* **1995**, 69, 545.
(36) Kang, E. T.; Neoh, K. G.; Tan, K. L. *Phys. Rev. B* **1991**, *44*, 10461.
(37) Moulder, J. F.; Stickle, W. F.; Sobol, P. E.; Bomben, K. D. *Handbook of X-ray Photoelectron Spectroscopy*; Perkin-Elmer: Eden Prairie, MN, 1992; p 63.
(38) Ruiz, J. P.; Nayak, K.; Marynick, D. S.; Reynolds, J. R. *Macromolecules* **1989**, *22*, 1231.
(39) Gallazzi, M. C.; Castellani, L.; Marin, R. A.; Zerbi,G. *J. Polym. Sci., Part A, Polym. Chem.* **1993**, *31*, 3339.
(40) Russo, M. V.; Polzonetti, G.; Furlani, A. *Synth. Met.* **1991**, *39*, 291.

MA0015018